luisacap@bu.edu
(1)Boston University, CSP
(2)UCLA
(3)University of Texas
(4)University of Colorado Boulder

Characterizing the EMIC-Driven Electron Precipitation and its Effects in the Upper Atmosphere: Preliminary Results

Luisa Capannolo[1]
W. Li[1], Q. Ma[1,2], M. Qin[1], X. Shen[1], V. Angelopoulos[2], A. Artemyev[2], X. Zhang[2,3], . M. Hanzelka[1], R. Marshall[4], G. Berland[4]

1. INTRODUCTION, MOTIVATION, GOALS

Magnetospheric EMIC (electromagnetic ion cyclotron) waves can pitch-angle scatter radiation belt electrons into the Earth's atmosphere (precipitation). Our understanding of EMIC-driven precipitation is limited by the capabilities of available LEO satellites (e.g., POES, FIREBIRD).

Figure 1: Wave-driven precipitation

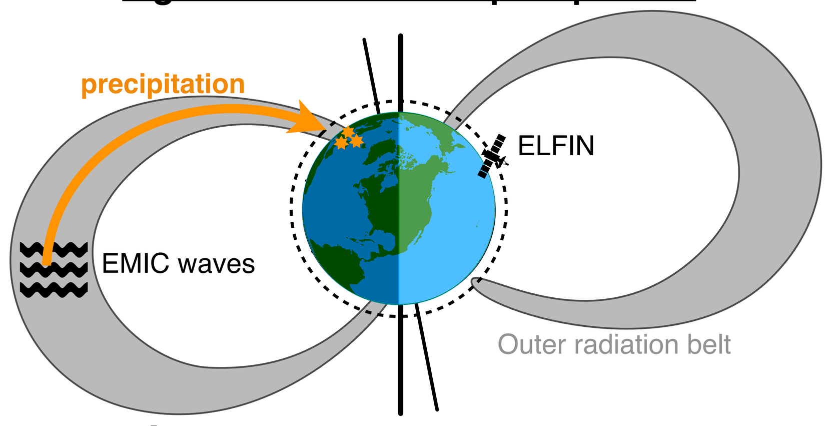

Electron precipitation can influence **Space Weather**:

- Leads to **reduction of the near-Earth radiation environment**
- Is a **source of energy input** into the atmosphere
- **Alters atmospheric ionization, conductivity and chemistry** (possibly contributing to ozone reduction)

Characterizing the typical properties of EMIC-driven precipitation and its associated ionization rates is essential to quantify the Space Weather effects of this phenomenon. We will:

1. Identify the location and radial extent of EMIC-driven precipitation
2. Describe the precipitation efficiency as a function of energy
3. Characterize the pitch-angle distribution inside the loss cone
4. Estimate the ionization rates of EMIC-driven precipitation

2. DATA and METHODOLOGY

ELFIN CubeSats:

- In LEO (~450km) over 2019-2022
- 0°–180° local pitch-angle coverage
- 60 keV–6 MeV electron energy range
- 3s time resolution

POES/MetOp constellation:

- In LEO (~850km) over 2012-now
- 0° & 90° look directions
- 10s–100s keV proton energy range
- 2s time resolution

Typical signature of EMIC-driven precipitation: ~MeV electron precipitation nearby (ΔL≤1.5; ΔMLT≤3) proton precipitation (well-known signature of EMIC wave activity)

Dataset: 144 precipitation events observed by ELFIN

Ionization rates: estimated using the BERI model (Boulder Electron Radiation to Ionization; [1]) with the observed averaged ELFIN pitch-angle distribution as input

3. EXAMPLE of EMIC-DRIVEN PRECIPITATION

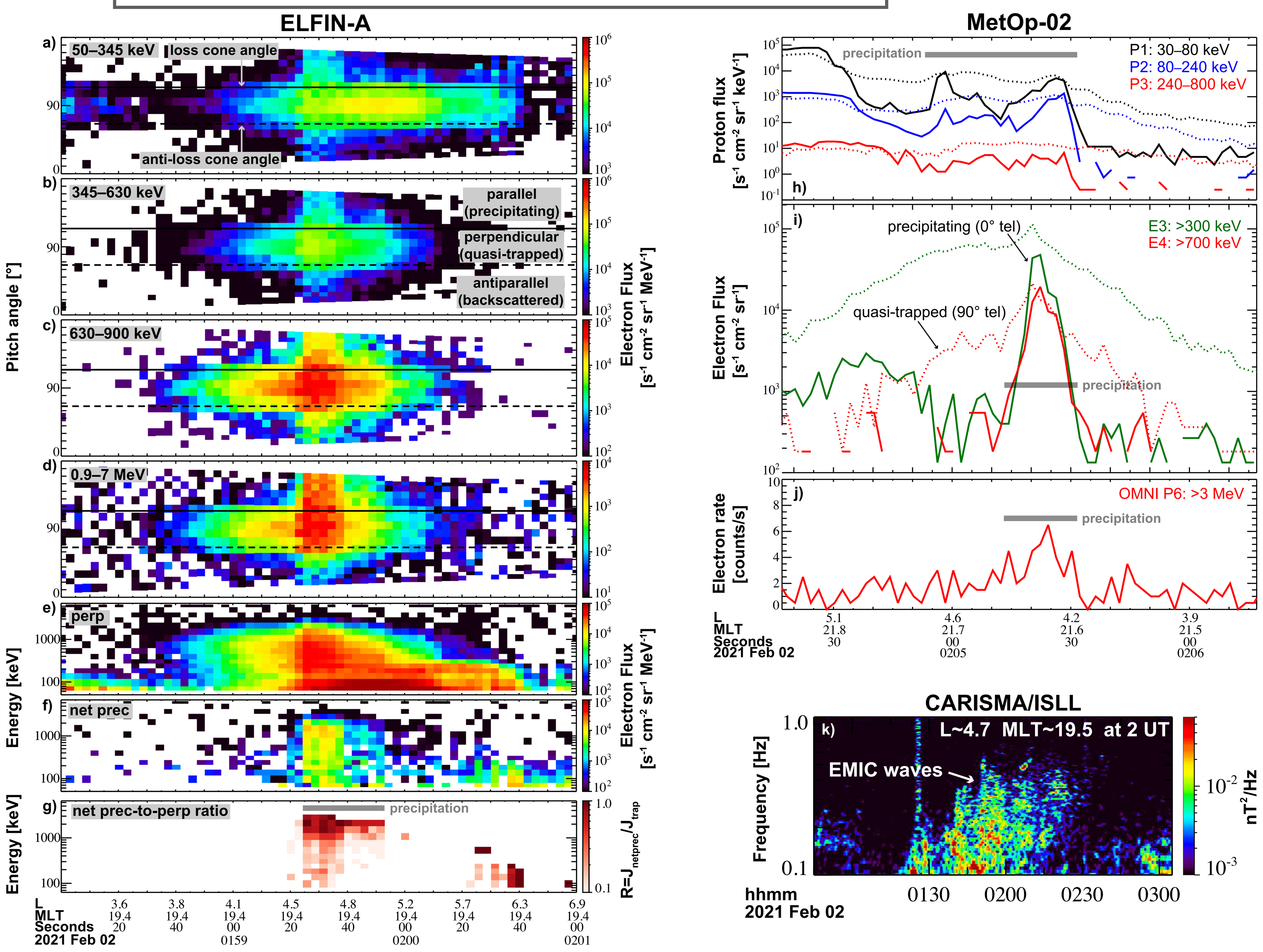

Figure 2: ELFIN-A: pitch-angle distribution (a-d), trapped (e) and precipitating (f) flux; ratio precipitating-to-trapped (g). MetOp-02: proton (h) and electron (i-j) flux at different energies. EMIC waves observed at ground (k).

EMIC-driven precipitation was observed by ELFIN-A and MetOp-02 in a similar L-MLT region as EMIC waves observed at ground. Precipitation was localized and occurred at 100 keV–3 MeV for electrons and 10s–100s keV for protons.

4. L-MLT DISTRIBUTION and PRECIPITATION EFFICIENCY

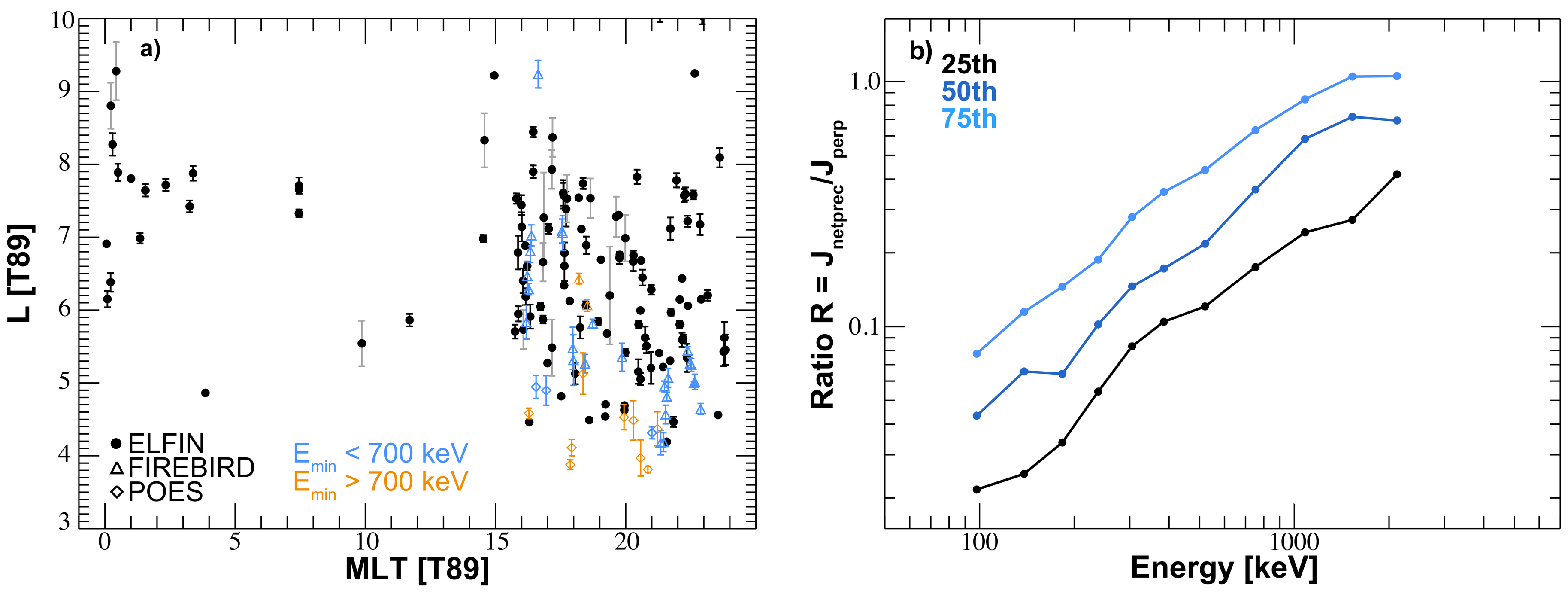

Figure 3: a) distribution of EMIC-driven precipitation from ELFIN (black), FIREBIRD and POES (from [2]); b) efficiency of precipitation (ratio precipitating-to-trapped R).

- Precipitation mainly occurs over 15–24 MLT and 5–8 L, but also extends towards dawn
- Precipitation is localized (average ΔL~0.3)
- Precipitation occurs from 100 keV–2 MeV, but the EMIC-scattering efficiency increases with energy

5. LOSS CONE DISTRIBUTION

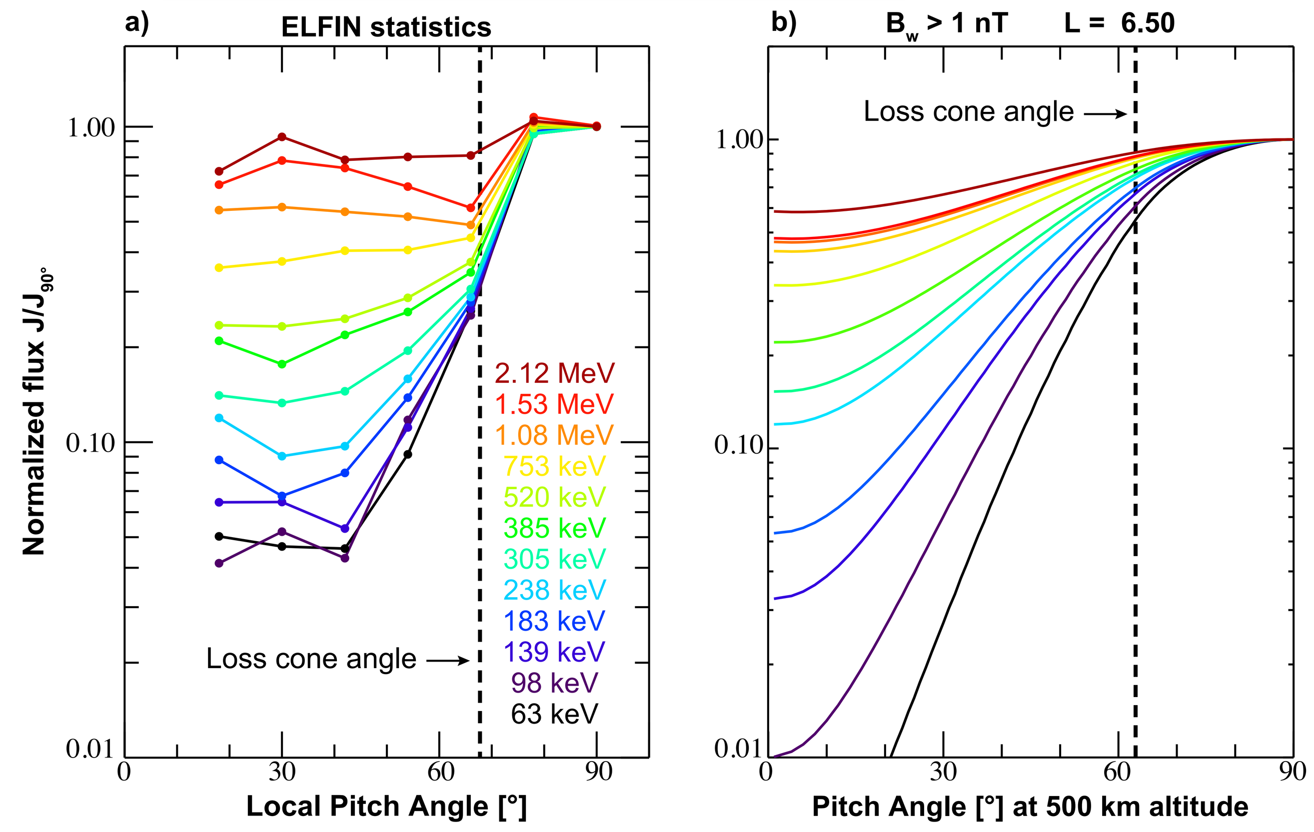

Figure 4: Pitch-angle distribution averaged from 144 EMIC-driven events (a) and from quasilinear simulations using EMIC wave statistics from [3].

- ELFIN's unprecedented pitch-angle resolution allows us to study the pitch-angle distribution within the loss cone
- EMIC waves fill up the loss cone with increasing energy
- Loss cone distribution from ELFIN's statistics agrees with the distribution obtained from quasilinear simulations using EMIC wave statistics

6. BERI INPUTS

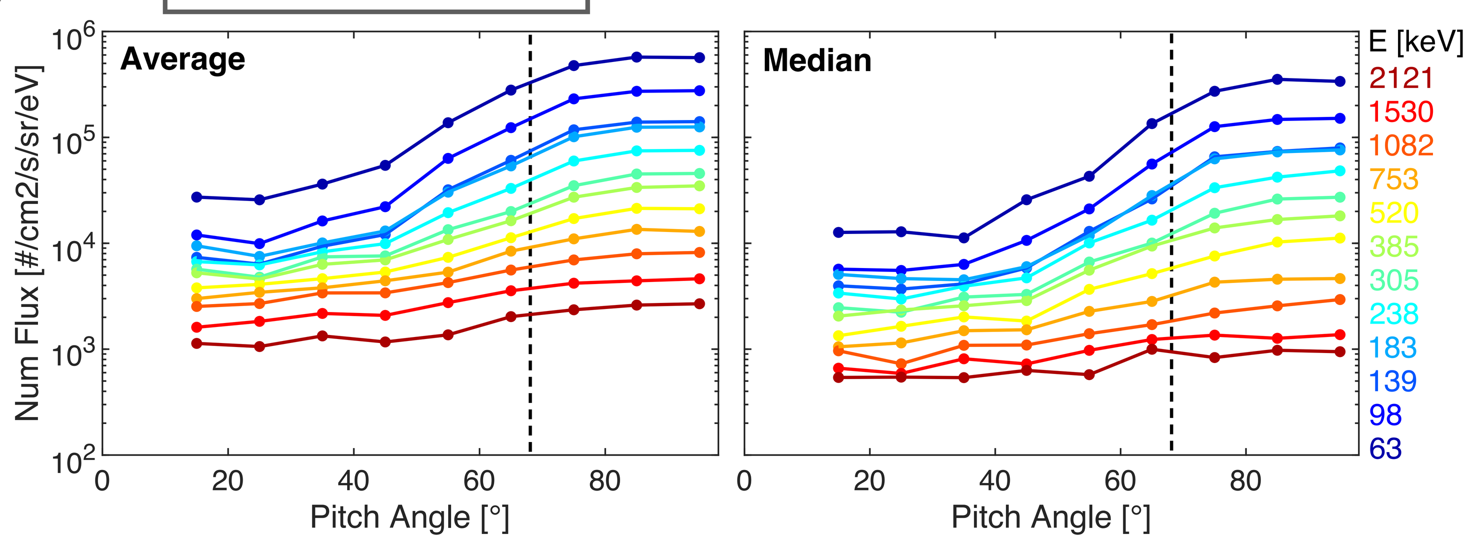

Figure 5: Average (left) and median (right) pitch-angle distribution of 144 EMIC-driven events.

- Average and median pitch-angle distribution of the EMIC-driven statistics from ELFIN are inputs to the BERI model (binned in 10° pitch-angles)
- Atmospheric density averaged on all 144 events (specifying latitude and longitude of ELFIN)

BERI tabulates the atmospheric ionization response to electrons (3 keV–33 MeV), fully accounting for the dependence of ionization production on background atmospheric density, electron energy, and pitch-angle.

7. IONIZATION RATES and DEPENDENCY on PITCH-ANGLE and ENERGY

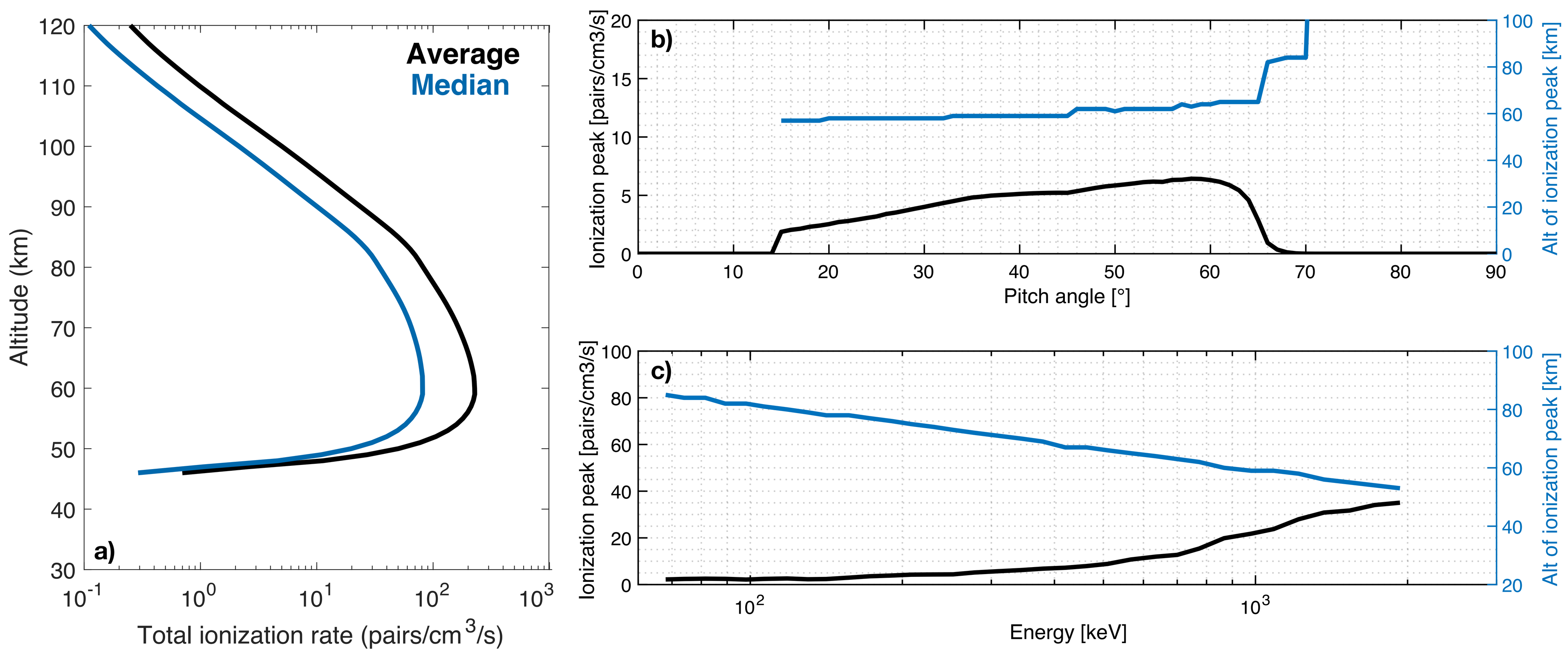

Figure 6: a) Atmospheric ionization rates for the average and median ELFIN distribution; ionization peak as a function of pitch-angle (b) and energy (c) in black; altitude corresponding to the ionization peak as a function of pitch-angle (b) and energy (c).

- Precipitation has a broad peak over 50–80 km
- The ionization peak increases as electrons are closer to the loss cone edge and increases as electrons are more energetic
- The altitude of the ionization peak has a weak dependence on pitch-angle, though more field-aligned electrons precipitate at lower altitudes
- The altitude of the ionization peak decreases with altitude because high-energy electrons can penetrate deeper in the atmosphere

8. CONCLUSIONS

- **EMIC-driven precipitation** is observed by ELFIN mainly over **15–24 MLT and 5–8 L**, with a **higher efficiency >700 keV** and weaker at 100s keV
- The BERI model is ideal to apply to ELFIN data, since ELFIN provides great coverage of the whole pitch-angle distribution
- EMIC waves drive **ionization rates of several 10s to few 100s pairs/cm³/s** over a broad altitude range (~ 50–80 km)
- The ionization is maximum for electrons at the loss cone edge and with ~MeV energies
- ~MeV electrons determine the highest ionization at ~55 km, while lower energy electrons deposit their energy at ~80 km

References:

1. Xu+2020: A generalized method for calculating atmospheric ionization by energetic electron precipitation. JGR: Space Physics. https://doi.org/10.1029/2020JA028482
2. Capannolo+2021: Energetic electron precipitation observed by FIREBIRD-II potentially driven by EMIC waves: Location, extent, and energy range from a multievent analysis. GRL. https://doi.org/10.1029/2020GL091564
3. Zhang+2016: Statistical distribution of EMIC wave spectra: Observations from Van Allen Probes. GRL. https://doi.org/10.1002/2016GL071158

Part of this work is under review in GRL. This research is supported by NSF (AGS-1723588, AGS-2019950, AGS-2247265) and NASA (80NSSC20K0698, 80NSSC20K1270, 80NSSC21K1385).